PROMOTIE INZICHT

Je staat op het punt om een wetenschappelijk onderzoek succesvol af te ronden. Het tastbare bewijs hiervan verdient alle aandacht. Promotie In Zicht helpt je graag het proefschrift voor jouw aanstaande promotie te realiseren.

You are about to successfully complete a scientific research. The tangible proof of your effort deserves all attention. Promotie In Zicht is happy to help with the design and formatting of your thesis.

Visualizing what is essential and bringing a thought to life

Harald Pieper

OVER MIJ | ABOUT ME

Zolang als ik me kan herinneren ben ik bezig met schetsen, tekenen en het verbeelden van mijn ideeën. Eerst op papier onder schooltijd, later tijdens mijn opleiding Grafisch Ontwerp aan de Academie voor Beeldende Kunsten in Breda, en aansluitend de opleiding Illustratie aan de Academie voor Beeldende Kunsten in Rotterdam. In 2007 heb ik In Zicht Grafisch Ontwerp opgericht. Ik werk voor diverse opdrachtgevers, en ik heb mij tevens gespecialiseerd in het vormgeven en opmaken van proefschriften.
Ieder proefschrift heeft zijn eigen verhaal en het is voor mij een mooie creatieve uitdaging om een ontwerp te maken dat echt aansluit bij de inhoud van het onderzoek en de wens van de promovendus.

As long as I can remember I have been sketching, drawing and imagining my ideas. First on paper during school hours, later during my Graphic Design study at the Academy of Arts Breda, and after that Illustration at the Academy of Arts Rotterdam. In 2007 I founded In Zicht Grafisch Ontwerp. I work for various clients and I am also specialized in the design and layout of theses. Each dissertation has its own story and it is a creative challenge for me to create a design that really matches the content of the research and the wishes of the PhD candidate.

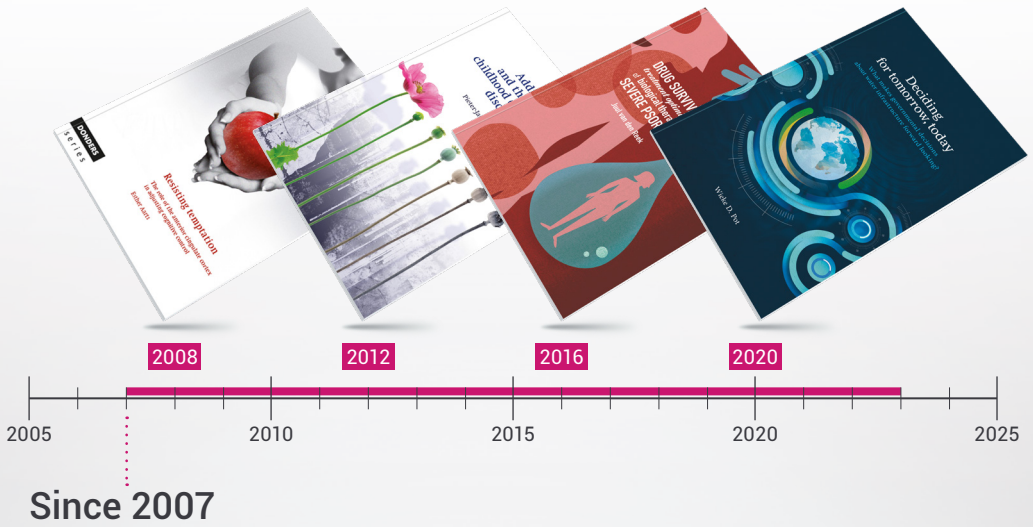

PROCES IN HET KORT | PROCESS IN SHORT

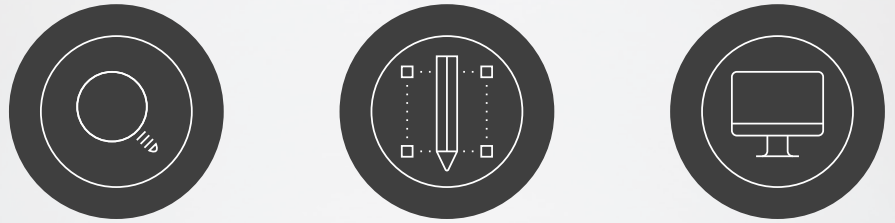

#1 CONCEPT
Idea of the design

#2 DESIGN
Working out the proposals

#3 REALIZATION
Layout to printing

Tijdens de briefing bespreken wij jouw wensen met betrekking tot concept, ontwerp en vormgeving van omslag en binnenwerk. Naar aanleiding hiervan ontvang je van mij de ontwerpvoorstellen. Voor het binnenwerk geldt dat er een ruim aanbod aanwezig is van verschillende lettertypen en layout-voorstellen. Zodra de vormgeving van het binnenwerk bepaald is zal er gestart worden met de opmaak. Na de auteurscorrecties worden de drukbestanden gemaakt en aangeleverd voor een eerste drukproef.
Bij akkoord op deze proef wordt de oplage gedrukt en ontvang je een complete PDF (binnenwerk + omslag) voor digitaal gebruik.

During the briefing we discuss your wishes regarding concept, design and realization of cover and inside. You will then receive the design proposals. For the inside, there is a wide range of different fonts and layout proposals. As soon as the design of the inside has been determined, the layout will be made. After the author's corrections, the print files are created and delivered for a first proof. If you agree with this proof, the books will be printed and you will receive a complete PDF for digital use.

CONTACT

06-28676851

info@promotie-inzicht.nl

Bezoekadres | **Visiting address**

Toernooiveld 100, 6525 EC Nijmegen

www.promotie-inzicht.nl

OFFER AND METHOD

Design and layout cover and bookmark

- Design and layout cover (based on briefing or supplied material), invitation/bookmark, author corrections up to and including print ready delivery PDF.
- Cover: sketch rounds, additional/adapted proposals (following the response to the draft), front and back, chapter pages, correction round and ready for printing.
  Optional: inside cover, extra invitation(s).

For the cover applies further:

- First a briefing
  (short list of questions)
  and possibly debriefing
- Start design
  (minimum of 5 proposals)
- Designs in trial
- Number of adapted proposals
  (depending on response to
  the designs)
- Correction round(s)
- Prepare files

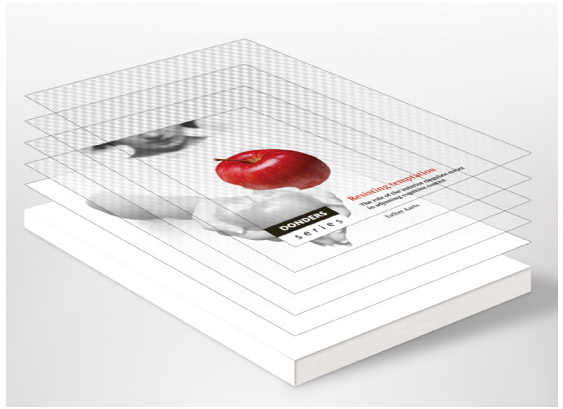

The briefing can be done by telephone, email or by appointment.

Inside design and layout

- Includes: 12 font proposals (PDFs) and ± 15 layout / design proposals per font (Each PDF consists of 13 spreads (26 pages), combinations or additions are possible). Check and uniformize figures (text in correct font + line thickness). Design tables.
- Design comes first, among other things attention is paid to: hyphenation (as little as possible and only for words > 15 characters), not too much space between the words and not a single word on the next line or a single sentence on the next page.

Extra: including invitation, PowerPoint, online PDF

- Extra options: online publication, complete PDF (inside + cover), invitation for dinner or party, background PowerPoint presentation.

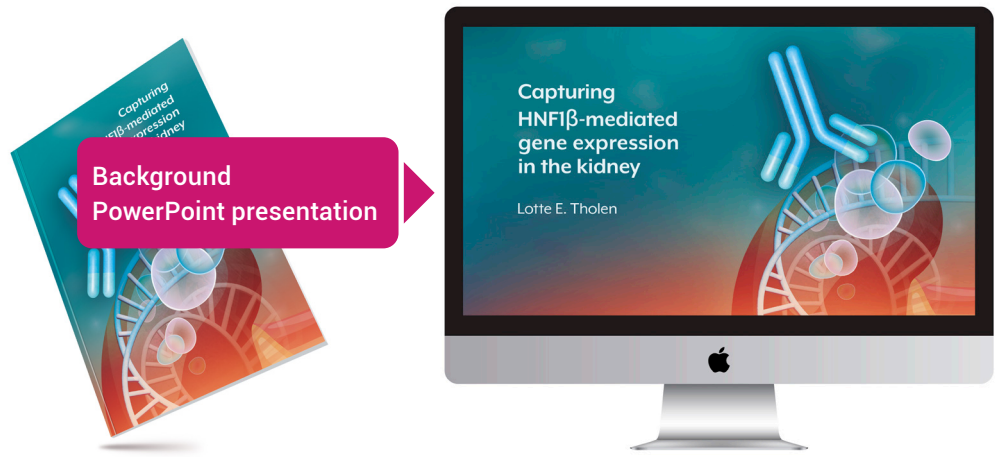

DIGESTING THE ROLE OF THE GUT MICROBIOME IN PROTON PUMP INHIBITOR (PPI)-INDUCED HYPOMAGNESEMIA

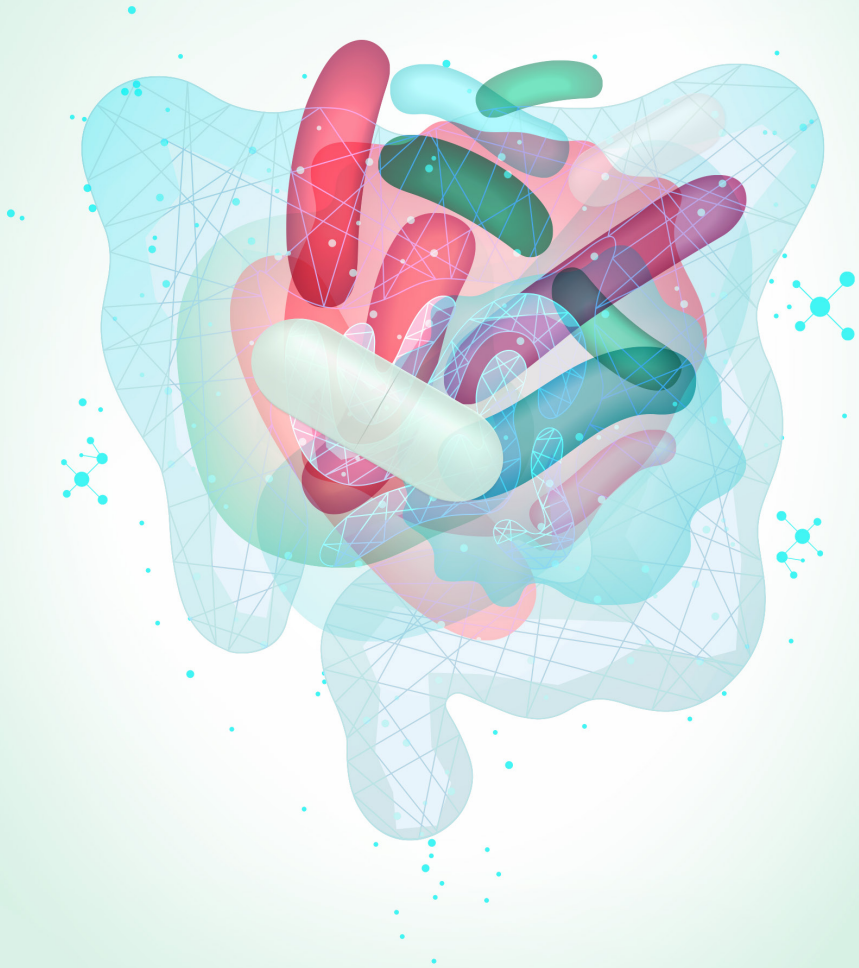

LISANNE M.M. GOMMERS

Example cover

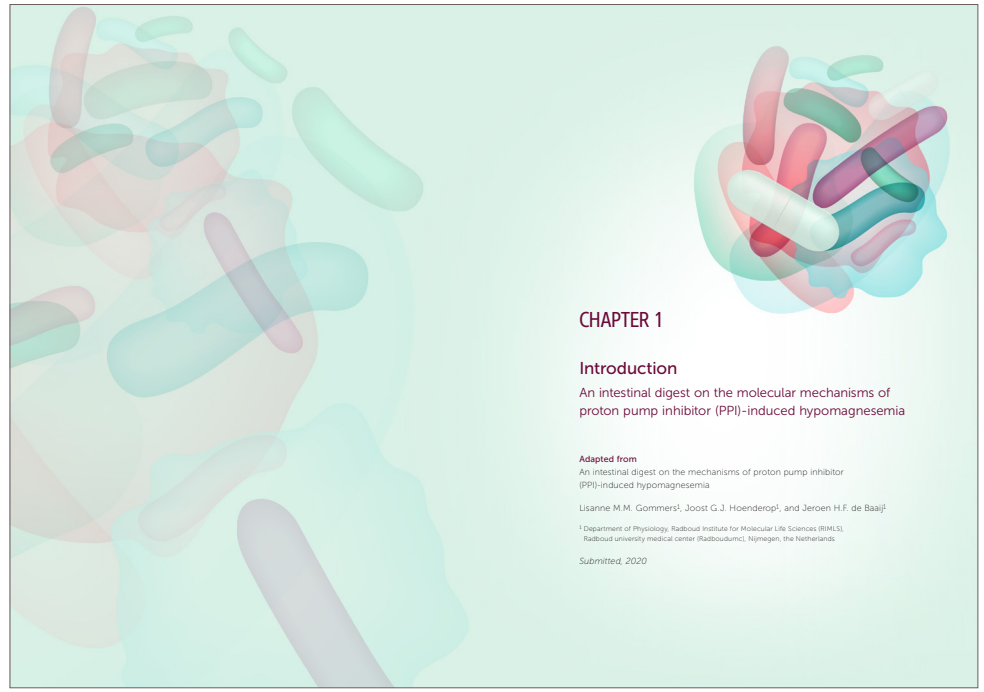

CHAPTER 1

Introduction

An intestinal digest on the molecular mechanisms of proton pump inhibitor (PPI)-induced hypomagnesemia

Adapted from
An intestinal digest on the mechanisms of proton pump inhibitor (PPI)-induced hypomagnesemia

Lisanne M.M. Gommers[1], Joost G.J. Hoenderop[1], and Jeroen H.F. de Baaij[1]

[1] Department of Physiology, Radboud Institute for Molecular Life Sciences (RIMLS), Radboud university medical center (Radboudumc), Nijmegen, the Netherlands

Submitted, 2020

Example chapter page

Results

Colonic butyrate concentrations negatively correlate with serum Mg^{2+} levels in mice

To assess whether microbiota-derived SCFAs influence Mg^{2+} homeostasis, correlation analyses were performed between colonic SCFAs concentrations and serum Mg^{2+} levels in wildtype C57BL/6J mice (**Figure 1**). In a previously published dataset, we measured the relative concentration of SCFAs in the colon of these mice [16]. Linear regression analysis showed a significant inverse correlation of colonic butyrate concentrations with serum Mg^{2+} levels ($P < 0.05$, $r^2 = 0.22$) (**Figure 1A**). No correlations were found between serum Mg^{2+} levels and colonic acetate or propionate concentrations (**Figure 1B-C**). This correlation was specific for Mg^{2+} as there was no correlation between colonic SCFAs concentrations and serum Ca^{2+} levels (**Figure 2**).

Butyrate reduces $^{25}Mg^{2+}$ uptake in Caco-2 cells

To explain the underlying mechanism of the inverse correlation between colonic butyrate concentrations and serum Mg^{2+} levels, we investigated whether butyrate affects Mg^{2+} uptake in the human colon cell line Caco-2 using the heavy ^{25}Mg isotope (**Figure 3**). Cells incubated for 20 minutes with 2, 4, or 8 mmol/L Na-butyrate had a significantly reduced $^{25}Mg^{2+}$ uptake compared to control (100 % vs. 88 % ± 2 vs. 86 % ± 4 vs. 72 % ± 3, respectively, $P < 0.05$) (**Figure 3A**). Of note, similar effects were observed with 8 mmol/L Na-propionate or Na-acetate (**Figure 4A**). The inhibitory effect of Na-butyrate was time-dependent, as 8 mmol/L Na-butyrate significantly lowered $^{25}Mg^{2+}$ uptake between 10- and 30 minutes compared to control-treated cells ($P < 0.05$) (**Figure 3B**). The inhibition by butyrate was specific for Mg^{2+} uptake, as there were no inhibitory effects on $^{45}Ca^{2+}$ uptake in Caco-2 cells (**Figure 4B-C**). Next, the fluorescent indicator magnesium green was used to assess whether butyrate could bind Mg^{2+} ions *in situ*. Na-butyrate (0-20 mmol/L) did not lower the $MgCl_2$ concentration in the presence of magnesium green (**Figure 3C**). As a control for our assay, we examined the binding of Mg^{2+} with ATP. Indeed, addition of 1 mmol/L ATP reduced the $MgCl_2$ concentration significantly by 2-fold (98 % ± 10 vs. 46 % ± 18, $P < 0.05$) and the fluorescent signal was abolished upon addition of 2 mmol/L ATP (**Figure 3D**). These results imply that butyrate does not lower the extracellular Mg^{2+} availability by direct interaction with Mg^{2+} ions. To determine whether the effects of butyrate were dependent on intracellular actions, butyrate uptake via the monocarboxylate transporter 1 (MCT1) was blocked by the known MCT1 inhibitor phloretin [17]. Similar to previous experiments, 20 minutes incubation with 8 mmol/L Na-butyrate significantly reduced $^{25}Mg^{2+}$ uptake (100 % vs. 65 % ± 5, $P < 0.05$) and this effect was abrogated by addition of 1 mmol/L phloretin (65 % ± 5 vs. 101 % ± 10, $P < 0.05$) (**Figure 3E**).

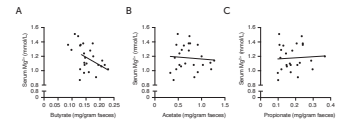

Figure 1. Butyrate concentrations in the colon negatively correlate with serum Mg^{2+} levels in mice. (**A-C**) Simple linear regression analyses were performed on colonic SCFAs concentrations, obtained from a previously published dataset [16], and serum Mg^{2+} levels of 25 wildtype male C57BL/6J mice. Simple linear regression analysis between colonic concentrations of butyrate ($y=-2.24x + 1.52$; $r^2= 0.22$, $P = 0.02$) (**A**), acetate ($y=-0.05x + 1.22$; $r^2 = 0.006$) (**B**), propionate ($y=0.15x + 1.15$, $r^2=0.003$) (**C**), and serum Mg^{2+} levels. Data is plotted as individual data points with the linear line indicating the relationship. $P < 0.05$ is considered significant.

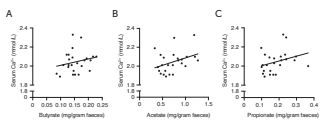

Figure 2. Colonic SCFAs concentrations do not correlate with serum Ca^{2+} concentrations. (**A-C**) Correlation analyses were performed on colonic SCFAs concentrations, as presented in a previously published dataset [16], and serum Ca^{2+} levels of 25 wildtype male C57BL/6J mice. Simple linear regression analysis between colonic concentrations of butyrate ($y=0.67x + 1.94$, $r^2= 0.05$) (**A**), acetate ($y=0.16x + 1.93$, $r^2 = 0.14$) (**B**), propionate ($y=0.50x + 1.96$, $r^2=0.10$) (**C**), and serum Ca^{2+} levels.

Example layout

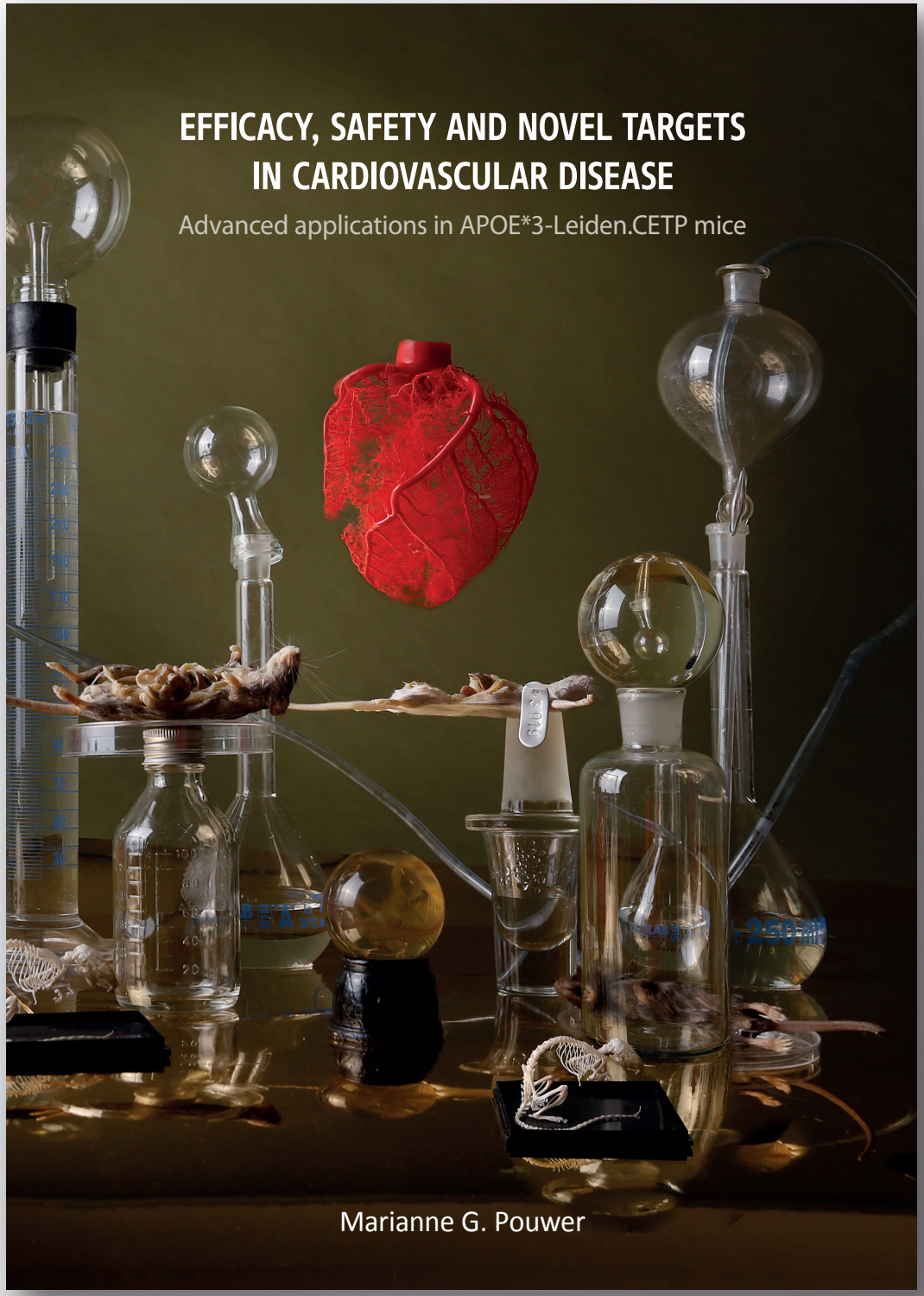

Example cover

Triple treatment with alirocumab and evinacumab on top of atorvastatin regresses lesion size and improves plaque phenotype in APOE*3-Leiden.CETP mice

Marianne G. Pouwer, Elsbet J. Pieterman, Nicole Worms, Nanda Keijzer, J. Wouter Jukema, Jesper Gromada, Viktoria Gusarova, Hans M. G. Princen

Submitted

Example chapter page

Abstract

Objectives: Regression of atherosclerotic plaque is modest with the current standard therapy, therefore it is beneficial to evaluate new therapeutic options. We investigated the effect of aggressive lipid-lowering interventions using double and triple treatment with simple or combined inhibition of PCSK9 and ANGPTL3 using the monoclonal antibodies alirocumab and evinacumab, respectively, on top of atorvastatin on regression of pre-existent atherosclerosis in APOE*3-Leiden.CETP mice.

Methods and results: Mice were fed a Western-type diet (WTD) for 13 weeks and thereafter matched into a baseline group (sacrificed at t=13), and 5 groups that continued to receive WTD alone or with treatment for 25 weeks: regression control, atorvastatin, atorvastatin and alirocumab, atorvastatin and evinacumab or atorvastatin, alirocumab and evinacumab. All interventions decreased plasma total cholesterol (-37% with atorvastatin to -80% with triple treatment, all p<0.001) by reduction of non-high-density lipoprotein cholesterol (non-HDL-C). Triple treatment decreased non-HDL-C levels at end-point from 10.7 mmol/L in control to 1.0 mmol/L (-91%, p<0.001). Mono-treatment with atorvastatin reduced the progression of atherosclerosis (-28%, p<0.001 vs control), double treatments completely blocked further progression and improved plaque stability, whereas triple treatment regressed lesion size in the thoracic aorta (-50%, p<0.05 vs baseline) and in the aortic root (-36%, p<0.05 vs baseline), diminished macrophage accumulation through reduced proliferation and further improved plaque stability.

Conclusions: This preclinical study using APOE*3-Leiden.CETP mice demonstrates that high-intensive cholesterol-lowering triple treatment with atorvastatin, alirocumab and evinacumab targeting all apoB-containing lipoproteins is a promising approach for regression of pre-existent atherosclerosis along with improvement in plaque phenotype.

Introduction

Atherosclerosis is the main cause of cardiovascular disease (CVD), and the annual number of deaths from CVD is predicted to rise from 17.5 million in 2012 to 22.2 million by 2030 (1). In addition to lifestyle changes (2), lipid-lowering has proven to be highly effective in reducing CVD, as every 1 mmol/L reduction in low-density-lipoprotein-cholesterol (LDL-C) is associated with a 23% CVD risk reduction (3). Since most patients at CVD risk are treated after development of atherosclerosis, therapies that regress pre-existent lesions are warranted.

Currently, statins are the 'golden standard' to lower LDL-C and to reduce CVD risk, but monotherapy with statins remains suboptimal as the achieved regression is modest, reflected by the small reductions in plaque volume (0.3-1.2% per year) (4,5). Furthermore, plaque regression is only seen in those patients with LDL-C reductions of >40% (6,7), or at plasma LDL-C levels below 78 mg/dL (2.0 mmol/L) (5,7), while a subgroup of patients still does not reach their LDL-C goals. Notably, the magnitude of regression is correlated with the percentage of LDL-C reduction (5,6), indicating the potential for further lipid-lowering. In this context, dual lipid-lowering therapies using ezetimibe or inhibition of proprotein convertase subtilisin/kexin type 9 (PCSK9) on top of a statin further reduce plaque volume relative to monotherapy with statins (5). While currently available therapies aim mostly to decrease plasma LDL-C, remnant cholesterol and triglyceride (TG) levels are considered to be an important residual risk factor for CVD as well (8,9). Actually, the clinical benefit of lowering TG and LDL-C may be proportional to the absolute change in apoB, implicating that all apoB-containing lipoproteins have approximately the same effect on the risk of CVD per particle (10). Therefore, novel high-intensive lipid-lowering or combination therapies targeting all apoB-containing lipoproteins may provide additional benefit to regress atherosclerosis and further reduce clinical events.

Since the severity and progression of coronary atherosclerosis are associated with adverse cardiovascular outcomes (4,11), the modest reduction in plaque volume achieved by statins cannot fully explain the reduced CVD risk, suggesting an important role for improved lesion stability (5,12,13). Animal models represent an opportunity to study plaque composition during regression. However, many mouse models have limited translational capability due to lack of responsiveness to lipid-lowering treatment (13). In this study we utilized APOE*3-Leiden.CETP mice, a well-established model with a human-like lipoprotein metabolism and atherosclerosis development (14) that responds well to hypolipidemic drugs (15–17).

We tested alirocumab and/or evinacumab on top of atorvastatin as high-intensive lipid-lowering strategy to evaluate their effect on regression of pre-existent atherosclerosis in APOE*3-Leiden.CETP mice. In addition, we assessed the effects on plaque composition and stability, and further looked into the process of macrophage reduction during regression. Alirocumab is a fully human monoclonal antibody to PCSK9 that reduces the

Example abstract

Table 1 Quantitative analyses of multiple inflammatory biomarkers using the Myriad RBM mouse inflammation multi-analyte profile

Marker*1	Neg. control		AT04A		AT04A vs control
	Mean (n=15)	SD	Mean (n=15)	SD	p-value
SCF (pg/mL)	1097.0	235.1	760.6	196.9	0.0002
VEGF-A (pg/mL)	549.1	66.5	246.8	75.5	0,0304
MIP-1 beta (pg/mL)	229.6	60.6	174.0	70.9	0.0319
MDC (pg/mL)	395.5	132.9	308.5	56.5	0.0397
M-CSF-1 (ng/mL)	9.3	1.6	8.2	1.0	0.0533
MCP-5 (pg/mL)	19.9	5.3	16.4	5.1	0.0552
IP-10 (ng/mL)	105.9	22.7	92.0	26.7	0.0848
MIP-3 beta (pg/mL)	3.6	1.3	3.0	0.8	0.1190
TIMP-1 Mouse (ng/mL)	1.7	0.8	1.4	0.3	0.2101
IL-18 (ng/mL)	34.5	12.4	35.1	7.9	0.2576
EGF Mouse (pg/mL)	189.7	30.1	179.7	17.2	0.3605
MCP-1 (pg/mL)	117.7	40.3	112.4	32.3	0.4427
MIP-1 alpha (pg/mL)	7.5	0.9	7.7	2.7	0.5066
MCP-3 (pg/mL)	215.7	83.7	207.2	37.1	0.6186
Thrombopoietin (ng/mL)	48.2	6.8	43.4	12.2	0,7400
IL-1 beta (ng/mL)	12.7	2.4	12.0	2.1	0.7996
Eotaxin (pg/mL)	434.0	90.8	450.7	138.0	0.8034

*1 the inflammatory markers FGF-9, FGF-basic, GM-CSF, KC/GRO, INF-gamma, IL-1 alpha, IL-2, IL-3, IL-4, IL-5, IL-6, IL-7, IL-10, IL-11, IL-12, IL-17A, LIF, MIP-2, OSM, TNF-alpha were measured, but were either below the limit of detection or the limit of quantification.

Table 2 Safety aspects of PCSK9 immunisation

	Body weight	Food intake	Liver weight	ALT	AST
	gram	*gram/mouse/day*	*gram*	*U/L*	*U/L*
Baseline	22.5 ± 1.2	3.4 ± 0.1	NA	80	141
Control	25.2 ± 2.7	2.7 ± 0.2	1.5 ± 0.4	69	251
AT04A	25.6 ± 2.8	2.5 ± 0.1	1.4 ± 0.3	74	289

No differences in body weight, food intake (per cage), liver weight, plasma ALT (pooled per group), and plasma AST (pooled per group) between the control and AT04A group at sacrifice (t=18 weeks). Data are presented as group means ± SD (n=14-15). Abbreviations: alanine transaminase (ALT), aspartate transaminase (AST).

Example tables

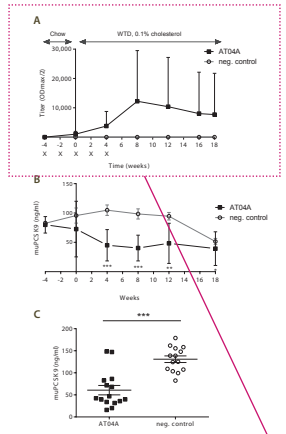

Figure 2 AT04A immunization induces a high and long-lasting immune response, and decreases plasma muPCSK9 levels. Antibody titres were assessed at different time points throughout the study. Crosses indicate the time points of the bi-weekly immunizations of control and AT04A vaccine (A). The muPCSK9 plasma concentration was determined at different time points throughout the study and compared to control (B–C). To compare AT04A and control treated group, the unpaired two-tailed Student's *t*-test was used, followed by the Mann–Whitney correction for non-parametric data. Data are presented as group means ± SD (n=15).*p<0.05, ***p<0.001.

PCSK9 highly varies between individual mice and no statistically significant differences in titres of t=4 to 18 weeks were found (**Figure 2A**). As expected, control immunized mice did not show any immune response against PCSK9 (**Figure 2A**). As evidence for a direct interaction between the induced anti-PCSK9 antibodies and the target protein, the plasma concentration of muPCSK9 in AT04A-treated vs. control immunized mice was determined over time (**Figure 2B and C**). At the immunization start (t=–4 weeks) the PCSK9 level in AT04A and control treated group was comparable. However, in t=4, 8, 12 and 18 AT04A vaccine treated mice showed a highly significant decrease in PCSK9 concentration of 57, 59, 49, and 24%, respectively (p<0.001, p<0.001, p=0.001, and p=0.029, respectively) (**Figure 2B**) demonstrating a consistent and long-lasting effectiveness of the AT04A vaccine (**Figure 2C**). Due to unknown reasons, the plasma PCSK9 level of control treated mice dropped in t=18 weeks, however, the difference between AT04A and control treated mice remained significant (**Figure 2B**).

AT04A decreases plasma TC and non-HDL-C levels in APOE*3-Leiden.CETP mice

Four weeks after the cholesterol-containing WTD was initiated, control immunized APOE*3-Leiden.CETP mice showed a strong increase of plasma TC level from 3.4 mmol/L (t=0 weeks) to 15.5 mmol/L (t=4 weeks), which remained elevated until t=18 weeks (12.1 mmol/L) (**Figure 3A**). In contrast, in the AT04A immunized mice a sustained reduction of plasma TC from t=0 weeks (2.8 mmol/L, p=0.002) to t=18 weeks (7.8 mmol/L, p=0.002) was observed (**Figure 3A**). Thus, cholesterol exposure over the whole time period of atherosclerosis inducing WTD (t=0 to 18 weeks) was decreased by 53% (p<0.001) in AT04A vs. control-treated mice (**Figure 3B**). The TC lipoprotein profile of pooled plasmas per group was determined by FPLC (**Figure 3C–F**). Plasma levels of HDL-C remained unaffected by AT04A vaccination, however the levels of non-HDL-C (VLDL and LDL) were clearly reduced (**Figure 3F–H**), indicating that the anti-PCSK9 vaccine may be a powerful therapeutic approach for long-term non-HDL-C/LDL-C management. A strong positive correlation between TC and plasma PCSK9 concentration was found (R^2=0.75; p<0.001) suggesting a specific and effective targeting of PCSK9 by AT04A vaccine.

AT04A reduces number, size, and severity of atherosclerotic lesions in the aorta

In order to assess the effect of AT04A on atherosclerotic development upon 18 weeks of WTD, the aortic root was isolated and the lesions as well as the lesion severity were determined. AT04A vaccine-treated mice showed a significantly reduced lesion area (–64%, p=0.004) (**Figure 4A**) and number of lesions per cross-section (–35%, p=0.037) (**Figure 4B**), compared with controls. Moreover, in AT04A-vaccinated mice a significant higher percentage of lesion-free area per section (+119%, p=0.026) was detected (**Figure 4C**). The lesion severity was categorized according to the American Heart Association guidelines

Example figure

All Tables are converted to the chosen design

All Figures are optimized: line thickness is made uniform, font type and size adjusted

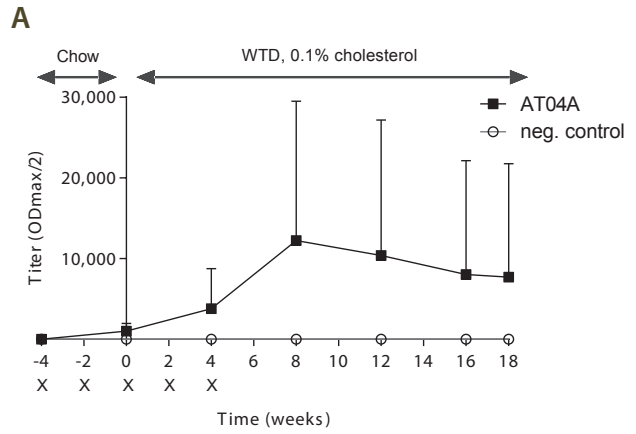

Fentanyl Pharmacokinetics

the role of clinical factors in patients with cancer
using transdermal or sublingual fentanyl

Evelien Kuip

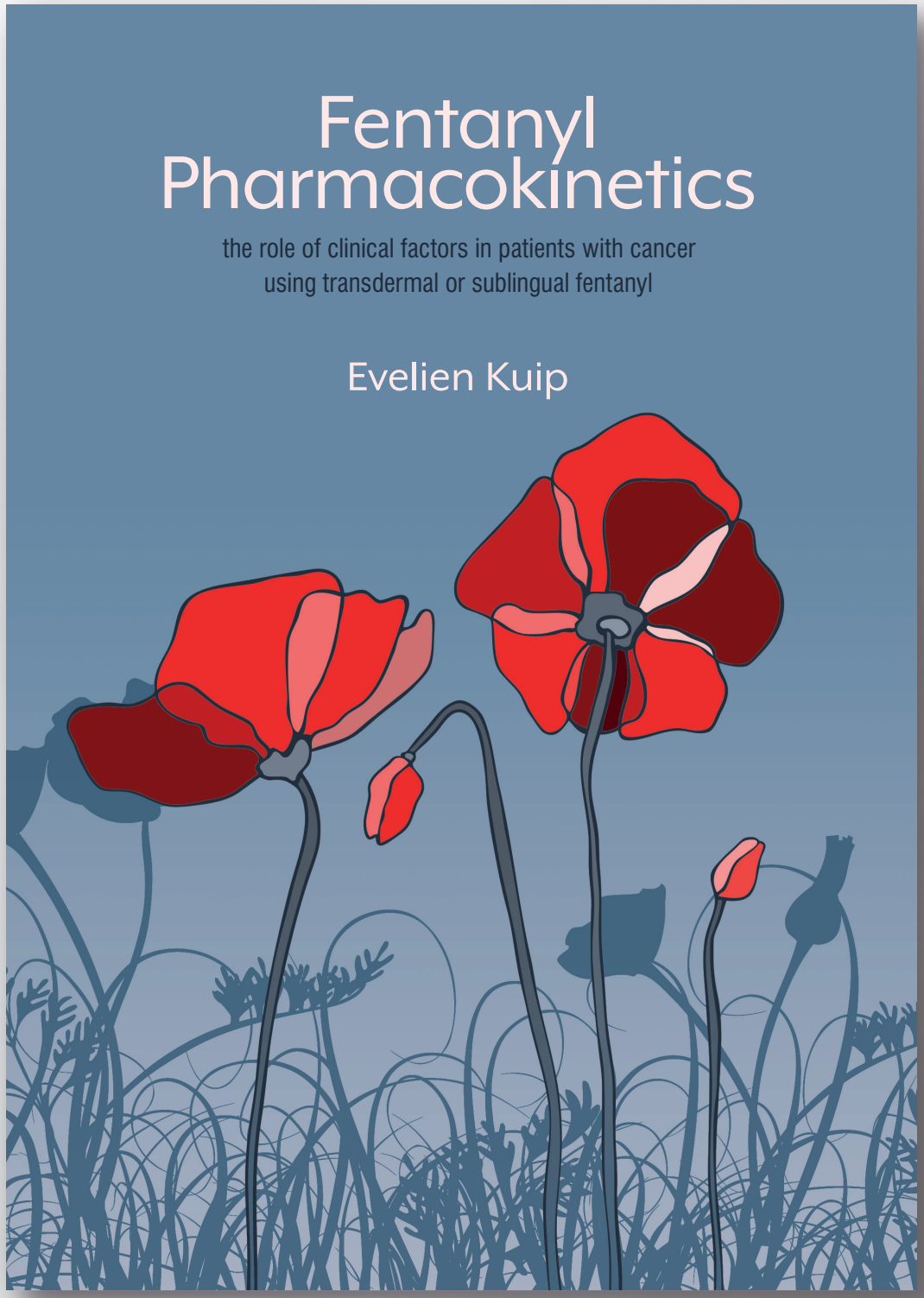

Example cover

2

A review of factors explaining variability in fentanyl pharmacokinetics; focus on implications for cancer patients

Evelien J.M. Kuip
Maarten L. Zandvliet
Stijn L.W. Koolen
Ron H.J. Mathijssen
Carin C.D. van der Rijt

Br J Clin Pharmacol. 83(2): 294-313, 2017.

Example chapter page

Table 2 Calculations of the between-run and within-run precisions and the average accuracy of the LLQ and QC samples[1]

Sample	Spiked (ng/mL)	GM (ng/mL)	ACC (%)	WRP (%)	BRP (%)	n[3]
Morphine						
LLQ	1.00	0.919	91.9	10.3	6.71	13 of 15
Low	3.00	2.88	96.0	7.92	8.67	14 of 15
Middle	40.0	38.1	95.3	3.60	4.50	15 of 15
High	80.0	77.5	96.9	2.23	1.76	15 of 15
Diluted	400	369	92.3	4.50	3.64	20 of 20
Morphine-3ß-glucuronide						
LLQ	10.0	8.40	84.0	5.16	≠[2]	13 of 15
Low	30.0	26.2	87.3	3.46	0.862	12 of 15
Middle	400	378	94.5	3.82	1.68	15 of 15
High	800	772	96.5	2.89	2.18	15 of 15
Diluted	4	3.824	95.6	1.79	≠[2]	15 of 15
Morphine-6ß-glucuronide						
LLQ	2.00	1.74	87.0	16.2	9.12	12 of 15
Low	6.00	5.84	97.3	10.2	5.61	12 of 15
Middle	80.0	77.1	96.4	5.38	≠[2]	15 of 15
High	160	156	97.5	4.16	≠[2]	15 of 15
Diluted	400	422	105.5	5.16	≠[2]	14 of 15
Hydromorphone						
LLQ	1.00	0.862	86.2	6.58	≠[2]	13 of 15
Low	3.00	2.80	93.3	4.09	≠[2]	15 of 15
Middle	40.0	39.0	97.5	4.35	1.85	15 of 15
High	80.0	77.9	97.4	1.87	≠[2]	15 of 15
Diluted	400	364	91.0	3.23	5.58	17 of 20
Fentanyl						
LLQ	0.100	0.0888	88.8	5.52	6.12	14 of 15
Low	0.300	0.269	89.7	4.29	1.07	13 of 15
Middle	4.00	3.76	94.0	7.01	≠[2]	15 of 15
High	8.00	7.40	92.5	1.37	1.86	15 of 15
Diluted	40.0	35.4	88.5	2.91	4.15	17 of 20
Norfentanyl						
LLQ	0.200	0.199	99.5	16.3	14.6	13 of 15
Low	0.600	0.604	100.7	7.82	0.406	15 of 15
Middle	8.00	7.75	96.9	4.64	≠[2]	15 of 15
High	16.0	15.3	95.8	3.86	≠[2]	15 of 15
Diluted	80.0	73.9	92.4	3.64	≠[2]	20 of 20

Abbreviations: GM, grand mean; WRP, within-run precision; BRP, between-run precision; ACC, average accuracy;
1, n=5 in 3 separate runs (4 runs at the QC Diluted for morphine, hydromorphone, fentanyl and norfentanyl)
2, no additional variation observed by performing the assay in different runs.
3, number of individual samples falling within acceptable range of accuracy of 85-115% (80-120% at LLQ)

Table 3 Calculations of carry-over, recovery and matrix factor

	Carry-over (%)	REC (%)	CV (%)	Matrix factor	CV (%)
Morphine	5.5	67.4	6.8	1.43	12.1
Hydromorphone	10.5	60.5	8.5	1.47	15.3
Fentanyl	4.8	85.4	3.0	1.04	3.3
Norfentanyl	0.28	72.4	9.5	1.21	13.3
M3G	0.53	82.5	1.9	1.21	16.3
M6G	2.7	121	18.2	1.54	4.5

The stability of morphine, hydromorphone, fentanyl and norfentanyl and the metabolites morphine-3ß-glucuronide and morphine-6ß-glucuronide was tested in triplicate at the concentrations of QC Low, QC-High and QC-Diluted. QC-samples were incubated for 18 hours at ambient temperature and stability was tested after three freeze-thaw cycles. All tested drugs showed to be stable under these circumstances.

Hydromorphone, morphine, fentanyl and norfentanyl were stable in potassium EDTA plasma for at least 76 months when stored at T<-70°C. Morphine-3ß-glucuronide and morphine-6ß-glucuronide were stable for at least 39 months when stored at T<-70°C (Table 4). All compounds showed to be stable as processed sample in the autosampler for at least 17 hours.

The described analytical methods were applied to clinical studies to investigate the pharmacokinetics of opioids. A representative concentration-time curve of a cancer patient receiving several opioids is presented in figure 2.

Example layout

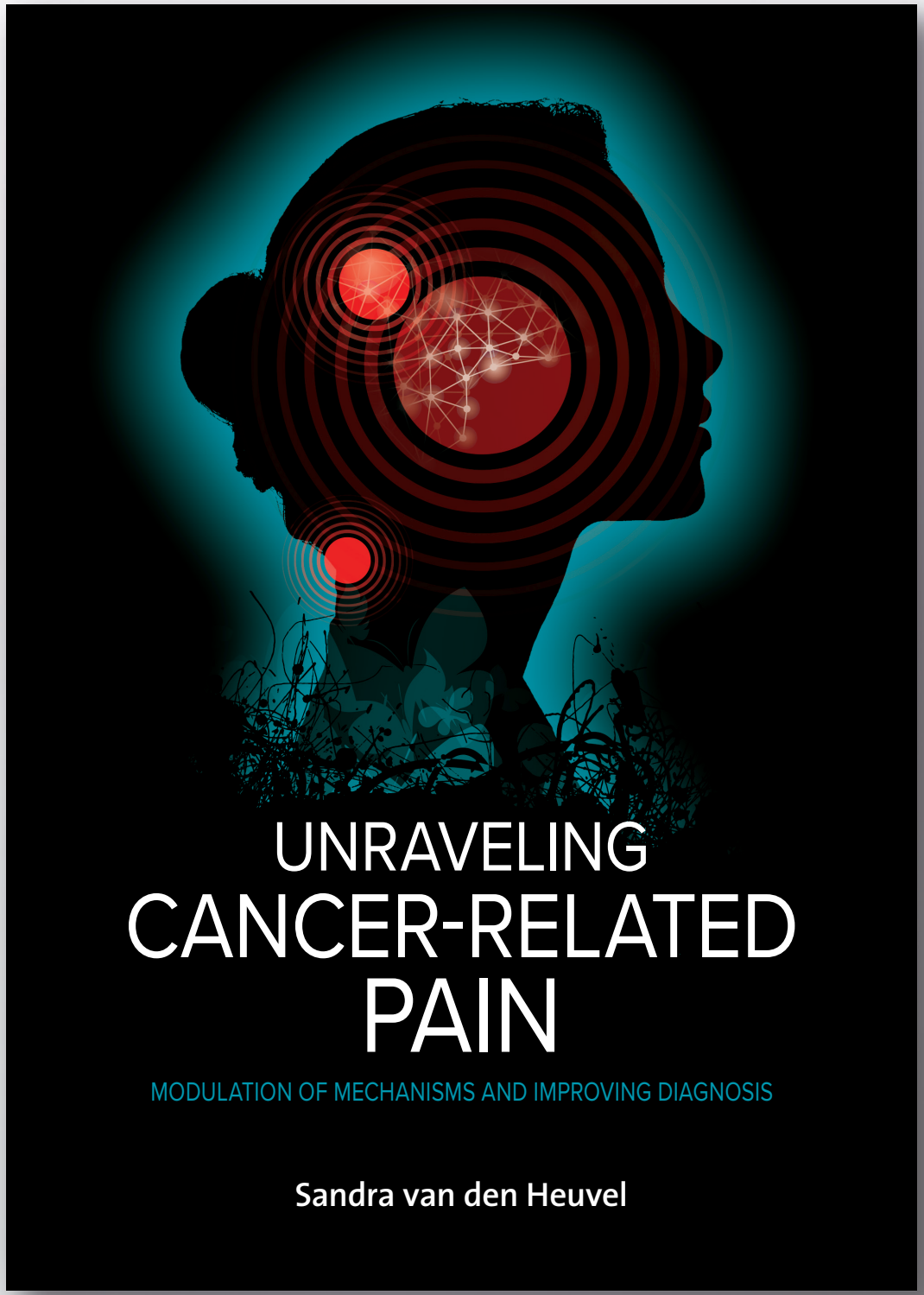

Example cover

pressure pain thresholds (PPT) and associated NRS scores is shown in Table 3. There was no significant effect of iv lidocaine on the mean PPT and associated NRS score. The effect on PPT before and after iv lidocaine varied between -2.31 to 1.16 N·cm^{-2} (P = 1); and for associated NRS score the effect varied between -0.67 to 0.06 NRS points (P = 0.204 - 1).

Table 3. PPTs and associated NRS scores before and after treatment with iv lidocaine.

	Location	Before *	After *	Effect	T-statistic	95% CI	P-value **
PPT	M. trapezius pars medialis	51.7 (14.3)	52.0 (12.5)	0.34	- 0.086	(- 9.6 - 8.9)	1
	Thenar eminence	58.0 (18.2)	58.3 (14.9)	0.33	- 0.070	(- 11.4 - 10.7)	1
	M. rectus femoris	71.3 (26.4)	69.0 (16.2)	- 2.31	0.257	(- 18.5 - 23.1)	1
	M. abductor hallucis	55.6 (27.7)	56.8 (18.3)	1.16	- 0.192	(- 15.0 - 12.7)	1
NRS	M. trapezius pars medialis	5.6 (2.0)	5.4 (2.4)	- 0.11	0.187	(- 1.3 - 1.5)	1
	Thenar eminence	5.6 (1.9)	5.1 (1.8)	- 0.56	2.294	(- 0.0 - 1.1)	0.204
	M. rectus femoris	4.9 (2.3)	5.0 (2.0)	0.06	- 0.127	(- 1.1 - 1.0)	1
	M. abductor hallucis	6.3 (2.0)	5.7 (2.0)	- 0.67	1.193	(- 0.6 - 2.0)	1

PPT: Pressure Pain Threshold, N·cm-2; NRS: Numeric Rating Scale, scale 0-10
* Data are expressed as means (SD); ** Bonferroni-corrected P values are reported

Thermal and mechanical sensory testing

Although individual patients could have an asymmetrical distribution of their stocking and glove distribution, no statistically significant difference was found between left and right side for the distribution of sensory changes for pinprick and cold in the whole group. Combining both limbs before and after lidocaine infusion, the cold detection level was significantly more caudal as the pinprick detection level (P = 0.008; difference = 6.1 cm; 95% CI 1.7 - 10.6) was found. For limbs and infusion separately, the pinprick detection level was always more cranial as the cold detection level; however in these subgroups with less observations the difference is not always statistically significant (P varies between 0.018 and 0.625). In 1 patient no changes in cold or pinprick sensation were observed.

Influence of lidocaine on thermal and mechanical sensory testing

The changes in distribution of pinprick and cold sensation in individual patients are presented in Table 4.

In 4 patients the area of abnormality in cold perception decreased after infusion. Three patients reported an increase in area in the upper or lower extremity after infusion. One patient showed a combination of positive change in one leg and a negative change in the other leg. The area of cold perception decreased when combining the limbs in all patients (P = 0.292; difference = 3.7 cm; 95% CI -3.5 – 10.8).

Table 4. The change in distance (Δ) for cold and pinprick stimuli before and after treatment with iv lidocaine.

	Cold				Pinprick			
	Arm		Leg		Arm		Leg	
Patient no.	Right Δ (cm)	Left Δ (cm)	Right Δ (cm)	Left Δ (cm)	Right Δ (cm)	Left Δ (cm)	Right Δ (cm)	Left Δ (cm)
1	- 22	- 14	- 45	- 3	- 28	- 22	- 30	- 41
2	0	- 26	- 8	- 2	0	+ 7	+23	+ 17
3	- 13	- 11	- 7	- 3	- 25	- 16	- 10	- 6
4	0	0	0	0	0	0	0	0
5	0	0	+ 24	+ 45	+2	-2	-2	- 3
6	0	0	0	+ 12	- 7	- 11	+ 27	+ 5
7	0	0	-8	-8	0	0	- 26	0
8	0	+ 19	+ 1	0	+ 19	+ 3	- 6	- 6
9	0	0	- 2	+6	0	0	-5	- 2

In 4 patients the area of abnormal pinprick sensation in the upper or lower extremities decreased after infusion, in 1 patient it increased in both upper and lower extremities. Three patients showed a combination of both increase in one area and decrease in another. The area of abnormal pinprick sensation decreased when combining the limbs in all patients (P = 0.099; difference = 6.4 cm; 95% CI -1.3 – 14.1).

Discussion

A single infusion of lidocaine decreased pain in 8 out of 9 patients with CIPN, which was correlated with duration of iv lidocaine infusion. The long-term analgesic effect of lidocaine was moderate with a mean duration of 23 days. Lidocaine had no effect on pain sensitivity measured by PPT. The distribution of sensory abnormalities was influenced by lidocaine.

There have been other studies that assessed the effect of iv lidocaine on neuropathic pain, but to our knowledge no study has specifically investigated the effect of lidocaine in CIPN. A Cochrane review that included 30 RCTs, showed that iv lidocaine and its oral analogues, mexiletine and tocainide, reduce neuropathic pain (9). This review included heterogeneous studies that looked at various etiologies of peripheral neuropathic pain (*e.g.* diabetic, posttraumatic, central pain) and lidocaine dosages also varied (1 – 5 mg·kg^{-1} in 30 – 60 minutes) between studies. Tremont-Lukats et al. investigated three dosing regimens of lidocaine (1, 3 and 5 mg·kg^{-1}·hr^{-1} during 6 hours) in various

Example layout

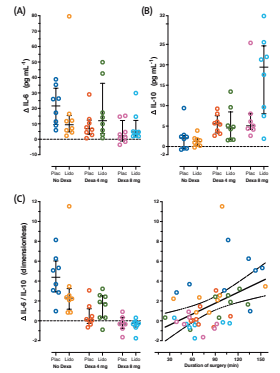

Figure 2. Difference (Δ) between interleukin (IL)-6, IL-10 plasma levels and ratio IL-6/IL-10 at baseline (t0) and those 4 hours after surgery (t2) in six groups (n=8 per group).

Each symbol represents one patient. A symbol above or below the zero line represents an increase or decrease, respectively, from t0 to t2. Error bars are the 25th-75th percentiles around the medians. (**a**) Observations for ΔIL-6 and (**b**) for ΔIL-10 per group. (**c**) Observations for the ratio ΔIL-6/IL-10 per group and linear regression of the pooled observations on the duration of surgery. The full regression line is accompanied with dotted lines showing its 95% confidence limits. There is one missing value in the group dexamethasone 8 mg with placebo for ΔIL-10 and ΔIL-6/IL-10. Plac = placebo, Dexa = dexamethasone, Lido = lidocaine.

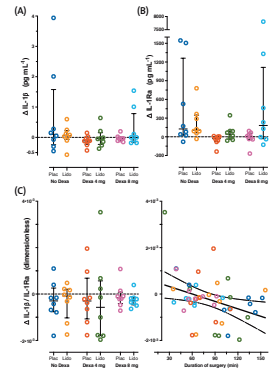

Figure 3. Difference (Δ) between interleukin (IL)-1β, IL1Ra plasma levels and ratio IL-1β/IL-1RA at baseline (t0) and those 4 hours after surgery (t2) in six groups (n=8 per group).

Each symbol represents one patient. A symbol above or below the zero line represents an increase or decrease, respectively, from t0 to t2. Error bars are the 25th-75th percentiles around the medians. (**a**) Observations for ΔIL-1β and (**b**) for ΔIL-1Ra per group. (**c**) Observations for the ratio ΔIL-1β/IL-1RA per group and linear regression of the pooled observations on the duration of surgery. The full regression line is accompanied with dotted lines showing its 95% confidence limits. Plac = placebo, Dexa = dexamethasone, Lido = lidocaine.

Example layout

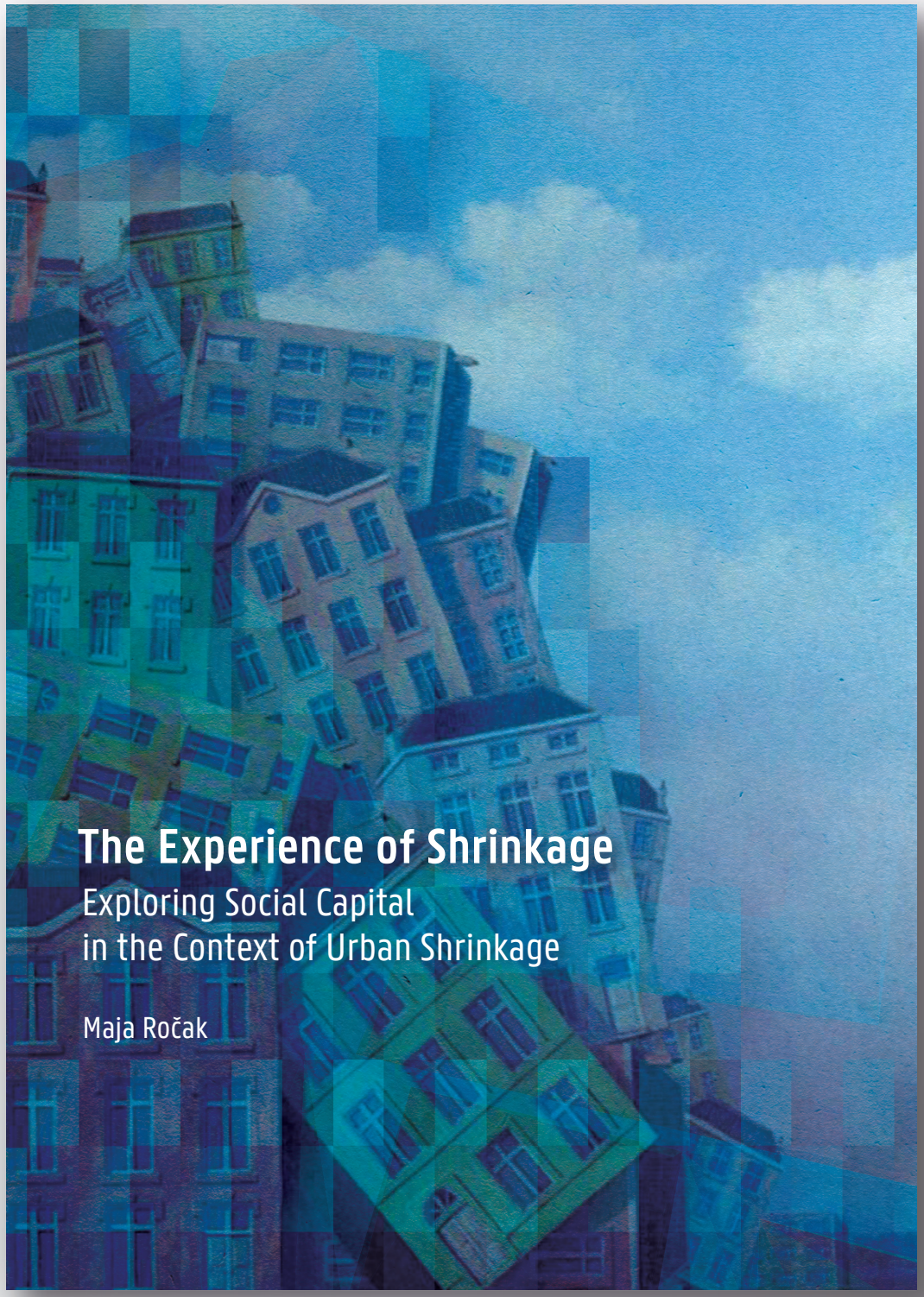

Example cover

Example chapter page

by the mining companies leading to a strong socio spatial dependency between the labour population and the mines (Peet, 2013). During this period, the Roman Catholic Church built strong ties with the mining companies and as such played an important role. The church and the mines shared the same interest: strong communities with obedient workers and social peace was very important (Hoekveld & Bontje, 2015; Peet, 2013).

The mining industry in Heerlen was terminated in 1965 by a decision of the Dutch government. This had serious consequences for Heerlen's population development and socioeconomic situation (Elzerman & Bontje, 2015; Verwest, 2011). In their heyday the mines employed 45,000 people directly and many more indirectly. Closures happened fast, but the mines' socioeconomic impact was underestimated as unemployment rates became twice the national average. Heerlen attempted to develop other industries to replace the employment generated by the mines but these attempts failed to match the skills of the population.

The first signs of population decline and selective out-migration began to be noticed around the 1990s and this trend is likely to continue in the future (Table 4). The factors influencing this development are not only economic and demographic, but also political and socio-cultural (Elzerman & Bontje, 2015). Shrinking has a selective character because of the brain drain of prosperous young people. Nevertheless, big differences within Heerlen can be observed: while some neighbourhoods are growing, other neighbourhoods are seriously shrinking[22] (Hoekveld & Bontje, 2015).

Table 4 Population prognosis for Heerlen (2000–2040).

Age	Year		
	2000	2015	2040
0-19	20 318	15 862	11 784
20-64	58 860	53 304	37 121
65+	15 969	18 631	24 318
Total	95 147	87 796	73 222

(Source: Etil, 2012)

22 In four (out of twenty three) neighborhoods the population grew (Bajdar, 2012).

Currently, Heerlen is a city with a low socioeconomic status, which means there are a large number of recipients of welfare provisions. In the annual Dutch statistics book, which compares the largest municipalities, Heerlen was compared with 49 other large municipalities in the Netherlands (Marlet & Van Woerkens, 2015). It shows that unemployment and poverty are higher than the national average. Additionally, Heerlen scores low on residential attractiveness (45th place out of 50) and in socioeconomic terms (44th place out of 50). It has a less highly educated labour force and a more deprived population, with more one-parent families and more people who are unable to work. Its poverty rate is higher than the national average (Marlet & Van Woerkens, 2015).

To enable a smooth transition from the mining era, to improve quality of life, and find a new identity for the city, many regeneration projects were and still are being conducted (Gemeente Heerlen, 2015b). After the closure of the mines the region wanted to start with a clean slate and transform from a black (mining) region to a green (park) city region Parkstad (Peet, 2013) with Heerlen as its centre. Mines were demolished to make way for abundant green areas. Heerlen is currently investing in different regeneration strategies aimed at maintaining or improving quality of life, economic performance, and sociocultural development (Gemeente Heerlen, 2015b).

3.4 Results and discussion

This study identifies three relevant indicators of social capital in shrinking cities, giving special attention to the experiences of citizens, analysed in the context of the Dutch shrinking city of Heerlen. The results reveal the prominence of three interrelated issues: the role of the local culture in all three social capital indicators; the lack of trust between citizens and politicians, and subjective experiences of urban shrinkage. In the following paragraphs we describe the main results of this study and compare them with the literature. If necessary, relevant quotes[23] from respondents are used to illustrate the results.

3.4.1 Shrinking city: A place called home with a bad image

Shrinking cities have limited economic, spatial, and natural resources (Pallagst et al., 2009). In this situation resources in the community or social resources, such as place attachment and trust, are deemed valuable for maintaining quality of life in the area. The idea is that it has a positive impact on social sustainability. Our

23 If deemed necessary, through the thesis relevant quotes from the interviewees are used to illustrate the results and are not meant to be generalisable. To guarantee anonymity, names of the interviewees have been changed.

Example layout

Illustration (image editing)

Illustration (vector/graphic)

Illustration (various techniques)

Illustration (various techniques)

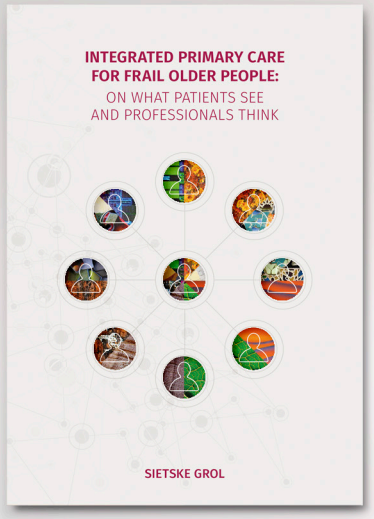

Special refinements: Die Cutting

Special paper: Cardboard

Illustration (vector/graphic)

Illustration (vector/graphic)

Illustration (vector/graphic)

Illustration (vector/graphic)

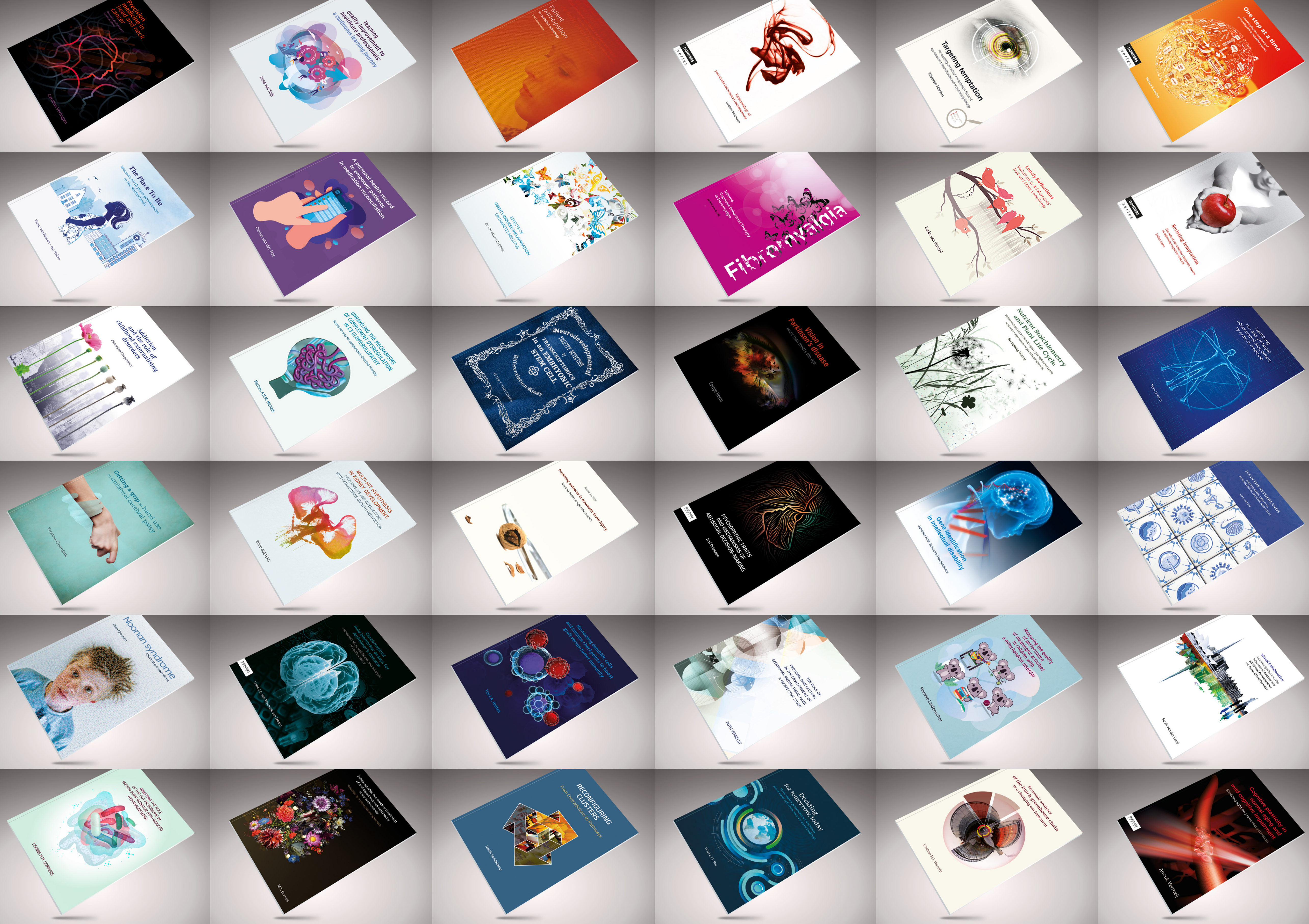

Precision medicine in head and neck cancer
Teaching quality improvement to healthcare professionals: a continuous learning journey
Patient participation
Targeting temptation
One step at a time
The Place To Be
A personal health record to empower patients in medication reconciliation
Fibromyalgia
Lonely Reflections
Resisting temptation
Addiction and the role of childhood externalising disorders
Neurodevelopmental toxicity testing by transcriptomics in an embryonic stem cell differentiation assay
Vision in Parkinson's disease
Nutrient Stoichiometry and Plant Life Cycle
Getting a grip on hand use in unilateral cerebral palsy
Predicting outcome in traumatic brain injury
Psychopathic traits and mechanisms of antisocial decision-making
Gene identification in intellectual disability
Noonan syndrome
Reconfiguring clusters
From Contradiction to Pathways
Deciding for tomorrow, today
Economic analyses of the Dutch greenhouse chain in a changing environment
Cognitive plasticity in normal aging and mild cognitive impairment

PROMOTIE INZICHT

CONTACT

06-28676851

info@promotie-inzicht.nl

Bezoekadres | **Visiting address**

Toernooiveld 100, 6525 EC Nijmegen

www.promotie-inzicht.nl